

## The Rb problem in massive AGB stars.

V. Pérez-Mesa<sup>1,2</sup>, D.A. García-Hernández<sup>1,2</sup>, O. Zamora<sup>1,2</sup>, B. Plez<sup>3</sup>, A. Manchado<sup>1,2,4</sup>, A.I. Karakas<sup>5,6</sup> and M. Lugaro<sup>6,7</sup>

<sup>1</sup> Instituto de Astrofísica de Canarias, E-38205 La Laguna, Spain

<sup>2</sup> Departamento de Astrofísica, Universidad de La Laguna, E-38206 La Laguna, Spain

<sup>3</sup> Laboratoire Univers et Particules de Montpellier, Université Montpellier2, CNRS, 34095 Montpellier, France

<sup>4</sup> Consejo Superior de Investigaciones Científicas, E-28006 Madrid, Spain

<sup>5</sup> Research School of Astronomy & Astrophysics, Australian National University, Canberra, ACT 2611, Australia

<sup>6</sup> Monash Centre for Astrophysics, Monash University, VIC3800, Australia

<sup>7</sup> Konkoly Observatory, Research Centre for Astronomy and Earth Sciences, Hungarian Academy of Sciences, 1121 Budapest, Hungary

### Abstract

The asymptotic giant branch (AGB) is formed by low- and intermediate-mass stars ( $0.8 M_{\odot} < M < 8 M_{\odot}$ ) in their last nuclear-burning phase, when they develop thermal pulses (TP) and suffer extreme mass loss. AGB stars are the main contributor to the enrichment of the interstellar medium (ISM) and thus to the chemical evolution of galaxies. In particular, the more massive AGB stars ( $M > 4 M_{\odot}$ ) are expected to produce light (e.g., Li, N) and heavy neutron-rich s-process elements (such as Rb, Zr, Ba, Y, etc.), which are not formed in lower mass AGB stars and Supernova explosions. Classical chemical analyses using hydrostatic atmospheres revealed strong Rb overabundances and high [Rb/Zr] ratios in massive AGB stars of our Galaxy and the Magellanic Clouds (MC), confirming for the first time that the  $^{22}\text{Ne}$  neutron source dominates the production of s-process elements in these stars. The extremely high Rb abundances and [Rb/Zr] ratios observed in the most massive stars (specially in the low-metallicity MC stars) uncovered a Rb problem; such extreme Rb and [Rb/Zr] values are not predicted by the s-process AGB models, suggesting fundamental problems in our present understanding of their atmospheres. We present more realistic dynamical model atmospheres that consider a gaseous circumstellar envelope with a radial wind and we re-derive the Rb (and Zr) abundances in massive Galactic AGB stars. The new Rb abundances and [Rb/Zr] ratios derived with these dynamical models significantly resolve the problem of the mismatch between the observations and the theoretical predictions of the more massive AGB stars.

## 1 AGB stellar nucleosynthesis

Low- and intermediate-mass stars ( $0.8 < M < 8$  solar masses) evolve towards the AGB just before they form planetary nebulae (PNe). At the end of the AGB phase, these stars experience thermal pulses (TP) and strong mass loss. The main processes of nucleosynthesis take place during the TP on the AGB. During this TP phase,  $^{12}\text{C}$  and heavy s-process elements (such as Rb, Zr, Sr, Nd, Ba, Tc, etc) are produced, enriching the ISM with specific isotopes (e.g., radionuclides).

Basically, at solar metallicity, we have that low-mass AGB stars ( $M < 1.5 M_{\odot}$ ) are O-rich and they probably do not form PNe. Intermediate-mass AGB stars ( $1.5 M_{\odot} < M < 4 M_{\odot}$ ) are C-rich and they do not experience hot bottom burning (HBB) and form s-process elements with  $^{13}\text{C}$  as neutron source. Finally, the high-mass AGB stars ( $M > 4 M_{\odot}$ ) remain O-rich because of the HBB activation and they produce s-elements the  $^{22}\text{Ne}$  neutron source. This evolutionary scenario has a strong dependence with the metallicity [2, 3, 4]. In short, the more massive AGB stars produce different elements than lower mass AGB stars and supernovae explosions and this maybe reflected in the gas and dust circumstellar chemistry.

In AGB stars, the  $^{13}\text{C}(\alpha, n)^{16}\text{O}$  and  $^{22}\text{Ne}(\alpha, n)^{25}\text{Mg}$  reactions can produce free neutrons to form heavy s-process such as Rb, Zr Sr, etc [1]. The  $^{13}\text{C}$  neutron source operates during the interpulse period and it is more efficient in low-mass AGB stars. On the other hand, the  $^{22}\text{Ne}$  neutron source operates at much higher neutron densities and higher temperatures during the convective thermal pulse. In the more massive AGB stars, the s-process elements are formed mainly via the  $^{22}\text{Ne}$  reaction. The  $^{22}\text{Ne}$  source strongly favors the production of  $^{87}\text{Rb}$  (also  $^{60}\text{Fe}$ ,  $^{41}\text{Ca}$ ,  $^{96}\text{Zr}$ ,  $^{25}\text{Mg}$ ,  $^{26}\text{Mg}$ ). The [Rb/Zr] ratio is a powerful indicator of the neutron density and, as such, is a good indicator of the stellar mass in AGB stars.

## 2 The Rb problem

We studied for the first time the more massive and O-rich AGB stars of our Galaxy and MC. These stars pertain to the so-called OH/IR stars and they display strong Rb overabundances with only mild Zr enhancements [2, 4] as expected from the  $^{22}\text{Ne}$  neutron source. The strong Rb enhancement ( $\sim 10\text{-}10^5$  times solar) confirms the activation of the  $^{22}\text{Ne}$  neutron source in massive AGB stars. The present AGB nucleosynthesis models can reproduce the observed correlation between the Rb abundances and the stellar mass and metallicity in the sense that increasing Rb abundances with increasing stellar mass and decreasing metallicity are theoretically predicted [7]; However, the standard theoretical models are far from matching the extremely high Rb abundances and [Rb/Zr] ratios seen in the more extreme stars [7]. This is, within the framework of the s-process it is not possible to overproduce Rb without co-producing Zr at similar levels.

A way to produce more Rb is the delay of the superwind phase in the more massive AGB stars. Indeed, massive AGB stars with delayed superwinds can produce more Rb than the standard models [5]. However, the delayed superwinds co-produce more Zr, so the theoretical

[Rb/Zr] ratio is very low.

There are two possible explanations for the Rb problem. First, if the high Rb and [Rb/Zr] ratios are real, then an unknown nucleosynthesis process is at work in the more luminous and extreme AGB stars. Second, the extremely high Rb enhancements and [Rb/Zr] ratios could be artifacts of the abundance analysis. So, the adopted model atmospheres (with hydrostatic equilibrium and LTE) likely fail to represent the real stars. More realistic model atmospheres (for example, models including a circumstellar envelope) are needed to address the discrepancy observed.

We have been working on the development of more realistic model atmospheres for extreme AGB stars. We started taking into account the presence of a circumstellar envelope. The next step would be the inclusion of dust in the models (which is more important in the infrared range) and to extend the hydrodynamical models to 3D.

### 3 Analysis using dynamical models

Our exploratory AGB wind models use a modified version of the Turbospectrum spectral synthesis code [6] to deal with extended atmospheres and velocity fields [8]. In these models, scattering is only included for the continuum and this approximation is consistent with complementary Monte Carlo simulations (only taking into account photon scattering for the radiative transfer) [8]. Our dynamical models are constructed from the original MARCS hydrostatic atmosphere structure, expanding the atmospheric radius by the inclusion of a wind out to about 5 stellar radii, with a radial velocity field in spherical symmetry and the stellar wind is computed under the assumptions of mass conservation and radiative thermal equilibrium, following a classical  $\beta$ -velocity law. In Figure 1 we show some examples of the  $\beta$ -velocity laws adopted in our dynamical models with different terminal velocity, mass-loss, and  $\beta$  exponent.

### 4 Results

The main result of our new dynamical models is that the effect of the circumstellar envelope is dramatic and the new Rb abundances are much lower (by one or two orders of magnitude) than those obtained with classical hydrostatic models. Also, the derived Rb abundances strongly depend on the expansion velocity and the mass-loss. This is shown in Figure 2, which displays the observed spectrum (black dots), the best hydrostatic model (blue line), the best dynamical one (red line) and other synthetic spectra for different mass-loss and velocity laws (green and cyan lines). The best dynamical model gives a Rb abundance that is 1.4 dex lower than the hydrostatic one. In addition, the dynamic models reproduce better the Rb line profile than the hydrostatic ones.

On the other hand, Zr is practically non affected by the presence of the circumstellar envelope and the [Zr/Fe] abundances with dynamical models are nearly to the solar values and very similar to those from the hydrostatic ones. This is because the ZrO band-head used

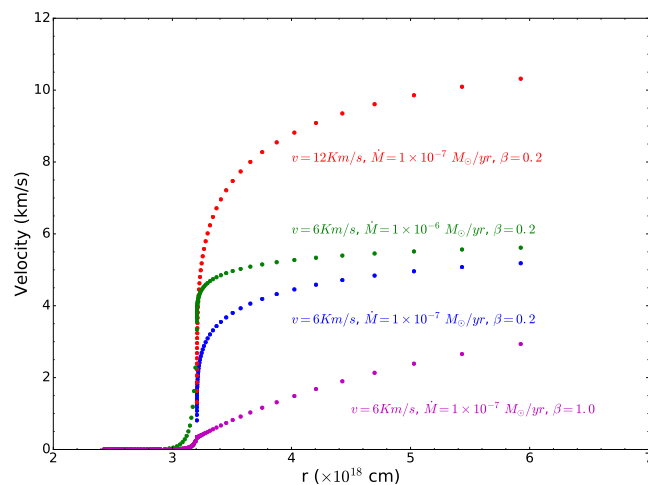


Figure 1: Velocity vs. distance from the star in four of our AGB wind models. The models are based on the MARCS hydrostatic model with effective temperature  $T_{eff} = 3000$  K, gravity  $\log g = -0.5$ , the solar chemical composition. These velocity laws present different terminal velocities  $v$ , mass-loss rates  $\dot{M}$  and  $\beta$  exponents.

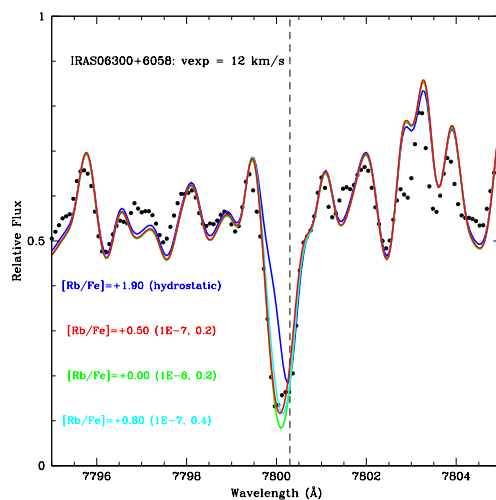


Figure 2: Rb I line profiles using dynamical models (red, green, and cyan lines), an hydrostatic model (blue line), and the observed spectrum (black dots) for the star IRAS 06300+6058.

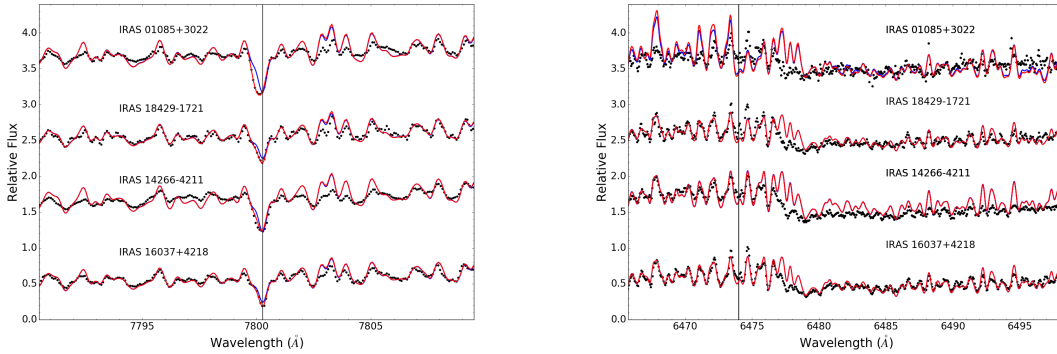


Figure 3: The Rb I 7800 Å (*left panel*) and ZrO 6474 Å (*right panel*) spectral regions in four massive Galactic AGB stars. The dynamical and hydrostatic models best fits (red and blue lines, respectively) to the observations (black dots) are shown. The location of the Rb I line and the ZrO bandhead are indicated by the green vertical lines.

in the chemical analysis is formed deeper in the atmosphere than Rb, being less affected by the circumstellar envelope. We can not distinguish the static models from the dynamic ones. In Figure 3 we display the observed Rb I (*left panel*) and ZrO (*right panel*) profiles in some massive AGB stars together with the best dynamical models (red lines) and the hydrostatic ones (blue lines).

In short, the Rb abundances and  $[\text{Rb}/\text{Zr}]$  ratios derived with the new dynamical models significantly resolve the problem of the mismatch between the observations of massive Rb-rich AGB stars and the theoretical predictions. In Table 1 we display the best fitting parameters of the dynamical models and the Rb and Zr abundances in four Galactic AGB stars and an extra-galactic one. The abundances obtained with the static models are also presented. The observations show Rb abundances between 0.0 and 1.0 dex and the  $[\text{Rb}/\text{Zr}]$  ratios in the galactic stars are in the range  $-0.3$  to  $0.7$ . This is in good agreement with both standard [7] and delayed superwind models [5]. However, still the extra-galactic star displays a too high  $[\text{Rb}/\text{Zr}]$  ratio.

## 5 Conclusion

In summary, the new Rb abundances and  $[\text{Rb}/\text{Zr}]$  ratios derived from more realistic AGB atmosphere models significantly resolve the present mismatch between the observations of massive AGB stars and the theoretical predictions. These dynamical models may find several applications; e.g., they can be applied to C-rich AGB stars or other types of stars with extended atmospheres. The circumstellar effects on other atomic lines like Li and Ca as well as on molecular lines such as CN and CO should be studied in the near future.

Table 1: Atmosphere parameters and abundances derived using dynamical models vs. hydrostatic models. The asterisk indicates that the  $T_{eff} = 3400$  K; in the other cases  $T_{eff} = 3000$  K.

IRAS name	$\log g$	$\beta$	$\dot{M}$ ( $M_{\odot} \text{ yr}^{-1}$ )	$v$ ( $\text{km s}^{-1}$ )	$[\text{Rb}/\text{M}]_{static}$	$[\text{Rb}/\text{M}]_{static}$	$[\text{Rb}/\text{M}]_{dyn}$	$[\text{Zr}/\text{M}]_{dyn}$
Galactic stars								
05098–6422	–0.5	1.0	$1.0 \times 10^{-8}$	6	0.1	$0.0 \pm 0.4$	$0.0 \pm 0.4$	$\leq 0.3 \pm 0.3$
06300+6058	–0.5	0.2	$1.0 \times 10^{-7}$	12	1.6	$1.9 \pm 0.4$	$0.5 \pm 0.7$	$\leq 0.1 \pm 0.3$
18429–1721	–0.5	1.0	$1.0 \times 10^{-8}$	7	1.2	$1.2 \pm 0.4$	$1.0 \pm 0.4$	$\leq 0.3 \pm 0.3$
19059–2219	–0.5	0.4	$1.0 \times 10^{-7}$	13	2.3/2.6	$2.4 \pm 0.4$	$0.8 \pm 0.7$	$\leq 0.3 \pm 0.3$
LMC star								
04498–6842*	0.0	1.0	$1.0 \times 10^{-7}$	13	3.9	$3.3 \pm 0.4$	$1.5 \pm 0.7$	$\leq 0.3 \pm 0.3$

## Acknowledgments

V.P.M. acknowledges the financial support from the Spanish Ministry of Economy and Competitiveness (MINECO) under the 2011 Severo Ochoa Program MINECO SEV-2011-0187. D.A.G.H. was funded by the Ramón y Cajal fellowship number RYC-2013-14182. V.P.M., O.Z., D.A.G.H. and A.M. acknowledge support provided by the Spanish Ministry of Economy and Competitiveness (MINECO) under grant AYA-2014-58082-P. M.L. is a Momentum (Lendlet-2014 Programme) project leader of the Hungarian Academy of Sciences. M. L. acknowledges the Instituto de Astrofísica de Canarias for inviting her as a Severo Ochoa visitor during 2015 August when part of this work was done. This paper made use of the IAC Supercomputing facility HTCondor (<http://research.cs.wisc.edu/htcondor/>), partly financed by the Ministry of Economy and Competitiveness with FEDER funds, code IACA13- 3E-2493.

## References

- [1] Busso, M., Gallino, R., & Wasserburg, G. J. 1999, ARAA, 37, 239
- [2] García-Hernández, D. A., García-Lario, P., Plez, B., et al. 2006, Science, 314, 1751
- [3] García-Hernández, D. A., García-Lario, P., Plez, B., et al. 2007, A&A, 462, 711
- [4] García-Hernández, D. A., Manchado, A., Lambert, D. L., et al. 2009, ApJ, 705, L31
- [5] Karakas, A. I., García-Hernández, D. A., & Lugaro, M. 2012, ApJ, 751, 8
- [6] Plez, B. 2012, Astrophysics Source Code Library, ascl:1205.004
- [7] van Raai, M. A., Lugaro, M., Karakas, A. I., García-Hernández, D. A., & Yong, D. 2012, A&A, 540, A44
- [8] Zamora, O., García-Hernández, D. A., Plez, B., & Manchado, A. 2014, A&A, 564, L4